Fish and Shellfish Immunology 92 (2019) 356–366

Contents lists available at ScienceDirect

Fish and Shellfish Immunology

journal homepage: www.elsevier.com/locate/fsi

Short communication

Molecular characterization and functional analysis of glutathione S-transferase kappa 1 (GSTκ1) from the big belly seahorse (*Hippocampus abdominalis*): Elucidation of its involvement in innate immune responses

Anushka Vidurangi Samaraweera[a], W.M Gayashani Sandamalika[a], D.S. Liyanage[a,b], Sukkyoung Lee[a,b], Thanthrige Thiunuwan Priyathilaka[a,**], Jehee Lee[a,b,*]

[a] Department of Marine Life Sciences & Fish Vaccine Research Center, Jeju National University, Jeju Self-Governing Province, 63243, Republic of Korea
[b] Marine Science Institute, Jeju National University, Jeju Self-Governing Province, 63333, Republic of Korea

ARTICLE INFO

Keywords:
Hippocampus abdominalis
glutathione S-Transferase
Innate immunity
Detoxification
Immune response

ABSTRACT

Glutathione S-transferases (GSTs) are essential enzymes for the bioactivation of xenobiotics through the conjugation of the thiol group of glutathione (GSH). In this study, a kappa class of GST was identified from the big belly seahorse (*Hippocampus abdominalis*) (HaGSTκ1) and its biochemical and functional properties were analyzed. HaGSTκ1 has 231 amino acids encoded by a 696 bp open reading frame (ORF). The protein has a predicted molecular mass of 26.04 kDa and theoretical isoelectric point (pI) of 8.28. It comprised a thioredoxin domain, disulfide bond formation protein A (DsbA) general fold, and Ser15 catalytic site as well as GSH-binding and polypeptide-binding sites. Phylogenetic analysis revealed that HaGSTκ1 is closely clustered with the kappa class of GSTs from teleost fishes. The recombinant (rHaGSTκ1) protein exhibited activity toward 1-chloro-2,4-dinitrobenzene (CDNB), 4-nitrobenzyl (4-NBC), and 4-nitrophenethyl bromide (4-NPB) but not 1,2-dichloro-4-nitrobenzene (DCNB). The optimum pH and temperature were 8 and 30 °C, respectively, for the catalysis of CDNB and the universal substrate of GSTs. The rHaGSTκ1 activity was efficiently inhibited in the presence of Cibacron blue (CB) as compared with hematin. Most prominent expression of *HaGSTκ1* was observed in the liver and kidney among the fourteen different tissues of normal seahorse. After challenge with lipopolysaccharide (LPS), polyinosinic-polycytidylic (poly I:C), gram-negative *Edwardsiella tarda*, and gram-positive *Streptococcus iniae*, *HaGSTκ1* expression was significantly modulated in the liver and blood tissues. Altogether, our study proposes the plausible important role of HaGSTκ1 in innate immunity and detoxification of harmful xenobiotics.

1. Introduction

Glutathione S-transferases (GSTs) are multifunctional enzymes that are primarily involved in cellular defense mechanisms against toxic compounds in most living organisms. Although the GSTs actively participate in prostaglandin D_2 synthesis [1], fatty acid β-oxidation [2], signal transduction pathway modulation, and ion channel production [3,4]. All living organisms produce energy from metabolic reactions to maintain their body homeostasis [5]. During these anabolic and catabolic pathways and as a result of exposure to the environment, organisms come in contact with metabolic wastes, toxic xenobiotics, reactive products, drugs, carcinogen metabolites, industrial pollutants, and insecticides. Cellular xenobiotic detoxification process plays a massive role to protect the body from these adverse compounds [6].

During detoxification, three main steps, namely phase I, phase II, and phase III, are involved in functionalization, conjugation, and elimination, respectively [7]. During phase I, compounds undergo modifications through oxidation, reduction, and hydrolysis reactions [8]. The functional groups such as COOH, OH, NH_2, and SH are converted to more polar forms with the action of cytochrome 450 enzyme and NADH cofactor [9,10]. The resulting reactive oxygen species produced may cause cellular damage and aging if these end products are not readily conjugated in phase II step [7]. Phase II is involved in the conjugation of products with enzymes such as GSTs,

* Corresponding author. Marine Molecular Genetics Lab, Department of Marine Life Sciences, College of Ocean Science, Jeju National University, 66 Jejudaehakno, Ara-Dong, Jeju, 690-756, Republic of Korea.
** Corresponding author. Marine Molecular Genetics Lab, Department of Marine Life Sciences, College of Ocean Science, Jeju National University, 66 Jejudaehakno, Ara-Dong, Jeju, 690-756, Republic of Korea.
E-mail addresses: thiunuwan88@jejunu.ac.kr (T.T. Priyathilaka), jehee@jejunu.ac.kr (J. Lee).

https://doi.org/10.1016/j.fsi.2019.06.010
Received 14 February 2019; Received in revised form 3 June 2019; Accepted 9 June 2019
Available online 11 June 2019

glucuronosyltransferases, methyltransferases, N-acetyltransferases, and sulfotransferases [10,11]. GSTs play an important role in the phase II detoxification process by catalyzing the conjugation of electrophilic substances with reduced glutathione (GSH) [12]. In this phase, the toxic compounds conjugate with GSH, acetyl coenzyme A, amino acids, and S-adenosyl-L-methionine via reactions of GSH conjugation, N-acetylation, and methylation, resulting in less toxic water-soluble compounds [7,11]. Finally, in phase III step, these soluble products are excreted through urine and feces by active transport.

The GST superfamily is broadly distributed in eukaryotes and prokaryotes. This protein family may be divided into three main subfamilies, including cytosolic GSTs, membrane-associated proteins involved in eicosanoid and glutathione metabolism (MAPEG), and plasmid-encoded bacterial fosfomycin resistance GSTs [13,14]. Based on their primary structures, immunological functions, substrate and inhibitor specificity, and chromosomal localization, the GSTs are divided into several groups, including alpha, beta, delta, mu, epsilon, phi, pi, lambda, zeta, sigma, theta, tau, and kappa [14,15]. GST proteins are biologically active as dimers and have an average molecular weight between 23 and 30 kDa for each subunit [14]. The basic secondary structure of GSTs shows that these proteins have a highly conserved G-site at the N-terminal domain and an H-site at the C-terminal domain with large structural changes. The N-terminal domain binds to GSH, whereas the C-terminal domain shows affinity toward different types of substrates [12,14,16].

The kappa class of GST is the least studied class among the other classes. Initially, kappa class was thought to belong to the theta class (θ); however, new kappa class evolved after the identification of glutathione transferase (13-13) from rat liver mitochondria [17]. Most studies with GSTs have focused on the biochemical characterization and expression level analysis after the pathogenic attack. Among aquatic organisms, the GST kappa from *Macrobrachium rosenbergii* [18] showed detoxification activity and response against biotic and abiotic oxidative stressors. An upregulation in GST kappa mRNA was observed in *M. rosenbergii* following bacterial (*Vibrio harveyi*) and viral (white spot syndrome virus) infections and heavy metal (cadmium) exposure [18]. The GST kappa from *Haliotis discus* showed responses against immune and stress challenges [19]. Moreover, the effect of a cyanobacterial crude extract on the transcription of GST kappa in different organs of *Carassius auratus* was studied [20]. Till date, very few studies have been performed on gene expression and functional analysis of the kappa class of GST as compared to other GST classes. No study has shown evidence on the functional analysis and immune response of the kappa class of GST from seahorse.

The big belly seahorse (*Hippocampus abdominalis*) belongs to the least concern category according to the IUCN red list of threatened species published in 2017 [21]. Habitat loss, degradation due to coastal development, and bycatch have resulted in the reduction in the big belly seahorse population. Furthermore, the exposure to toxic compounds, pathogenic agents such as bacteria, fungi [22], and parasites [23] has severely affected aquatic animals. Dried seahorses are traditional Chinese medicine in many countries, including China, Hong Kong, and Taiwan [24]. Therefore, seahorses are considered as biologically and economically valuable fish species. Analysis of immune protective genes such as those encoding GSTs are important to study the detoxification and conservative activities of seahorses against adverse situations in their living environment and to design effective approaches for the prevention of diseases. In this study, *HaGSTκ1* was identified from the seahorse cDNA database and subjected to molecular characterization. To determine the immune response of HaGSTκ1, the mRNA expression profile of *HaGSTκ1* was examined following challenge with lipopolysaccharide (LPS), polyinosinic-polycytidylic acid (poly I:C), *Edwardsiella tarda* (*E. tarda*), and *Streptococcus iniae* (*S. iniae*). Furthermore, the enzymatic properties of HaGSTκ1 were evaluated using the purified recombinant protein.

2. Materials and methods

2.1. Experimental seahorses and tissue isolation

Healthy juvenile seahorses were obtained from the Center of Ornamental Fish Breeding at Jeju Island, Republic of Korea. In order to determine the health conditions of the seahorses, we followed the guidelines for fish health and welfare monitoring [25]. The seahorses were acclimatized in laboratory aquarium tanks (300L) at 18 °C ± 2 °C and 34 ± 0.6‰ salinity at the Fish Vaccine Research Center, Jeju National University, for one week before the experiment. The seahorses were fed with Mysis shrimps before the experiment; challenged seahorses were not fed during experiment.

Tissues including blood, skin, kidney, ovary, spleen, heart, brain, testis, intestine, pouch, liver, gills, muscle, and stomach were isolated from six seahorses (3 males and 3 females) with ~12 cm average body length (average body weight 8 g) for tissue distribution analysis. Blood was obtained from the tail cutting, and the peripheral blood cells were separated by centrifugation at 3,000 × *g* and 4 °C for 10 min. The isolated tissues from six unchallenged seahorses were pooled separately by tissue type. All tissues were snap frozen in liquid nitrogen and stored at −80 °C until RNA extraction.

2.2. Challenge experiment

For the challenge experiment, 30 juvenile seahorses (average body weight 3 g) were divided into five groups, and each group were intraperitoneally injected with 100 μL of LPS (1.25 μg/μL) (Sigma, USA), poly I:C (1.5 μg/μL) (Sigma, USA), gram-negative *E. tarda* (5×10^3 CFU/μL), and gram-positive *S. iniae* (10^5 CFU/μL) suspensions prepared in PBS. For the control group, seahorses were injected with 100 μL of sterile PBS. After the injections, seahorses in each group were maintained in separate tanks under the same conditions (18 °C ± 2 °C and 34 ± 0.6‰ salinity). Blood and liver samples were collected at 0, 3, 6, 12, 24, 48, and 72 h post injection from five seahorses, as described in section 2.1. Tissues from five challenged seahorses from each group at different time points were pooled separately.

2.3. RNA extraction and cDNA synthesis

Total RNA was extracted using RNAiso plus total RNA extraction reagent (TaKaRa, Japan). RNA was purified with RNeasy Mini Kit (Qiagen, USA) and subjected to gel electrophoresis to evaluate quality. Concentrations were examined using Multiskan™ GO Microplate Spectrophotometer (Thermo Scientific, USA) at 260 nm wavelength. Complementary DNA (cDNA) was synthesized using 2.5 μg of RNA with PrimeScript™ II 1st strand cDNA Synthesis Kit (TaKaRa, Japan). cDNA was diluted 40 times in nuclease-free water and stored at −80 °C.

2.4. Identification and bioinformatic analysis of HaGSTκ1

The complete coding sequence of HaGSTκ1 was identified from the previously constructed seahorse transcriptome database [26] using Basic Local Alignment Search Tool (BLAST) tool of National Center for Biotechnology Information (NCBI) (https://blast.ncbi.nlm.nih.gov/Blast.cgi) [27]. The open reading frame (ORF) and amino acid sequence were determined using Unipro UGENE software [28]. ExPASy ProtParam tool (https://web.expasy.org/protparam/) [29] was used to determine the physiochemical parameters of HaGSTκ1. NCBI conserved domain database (https://www.ncbi.nlm.nih.gov/Structure/cdd/wrpsb.cgi) [30] and ExPASy PROSITE (https://prosite.expasy.org/) [31] were used to investigate the conserved domains of HaGSTκ1. Availability of signal peptide and N-glycosylation sites were predicted with SignalP 4.1 Server (http://www.cbs.dtu.dk/services/SignalP/) [32] and NetNGlyc 1.0 Server (http://www.cbs.dtu.dk/services/NetNGlyc/) [33], respectively. Pairwise sequence and multiple

Table 1
Primer sequences used in this study.

Name	Sequence (5′-3′)
HaGSTκ1 - qPCR Forward primer	CTTGGGCAGGAGCGAAATTGAAGAG
HaGSTκ1 - qPCR Reverse primer	CATCTCAGCTTTCCCGTTGATGTGG
HaGSTκ1 - cloning primers - Forward	GAGAGAgcggccgcATGACCTCCAAAAAGGTGATCGAGT – NotI
HaGSTκ1 - cloning primers - Reverse	GAGAGAgaattcTCACAGTTTGGCAGATGACCTTTCA – EcoRI
40s ribosomal protein S7 - qPCR internal control - Forward	GCGGGAAGCATGTGGTCTTCATT
40s ribosomal protein S7 - qPCR internal control - Reverse	ACTCCTGGGTCGCTTCTGCTTATT

Table 2
The specific activity of HaGSTκ1 for different substrates and substrate-specific parameters at 25 °C when substrate and GST enzymes were at 1.0 mM.

Substrate	pH	λ_{max} (nm)	Molar extinction coefficient (ε) ($mM^{-1}cm^{-1}$)	Specific activity (μmol.$min^{-1}mg^{-1}$ protein)
CDNB	6.5	340	9.6	0.26 ± 0.07
DCNB	7.5	345	8.5	ND
ECA	6.5	270	5.0	0.03 ± 0.012
4-NPB	6.5	310	1.2	1.70 ± 0.108
4-NBC	6.5	310	1.9	0.99 ± 0.05

sequence alignments were performed with EMBOSS Needle (https://www.ebi.ac.uk/Tools/psa/emboss_needle/) [34] and Clustal Omega (https://www.ebi.ac.uk/Tools/msa/clustalo/) [35] color align conservation (http://www.bioinformatics.org/sms2/color_align_cons.html) [36] tools, respectively. A phylogenetic tree was constructed by the neighbor-joining method with 5,000 bootstrapping replicate values using MEGA 6.0 [37]. The three-dimensional (3D) structure of the monomer and dimer of HaGSTκ1 was constructed using I-TASSER (https://zhanglab.ccmb.med.umich.edu/I-TASSER/) [38] and SWISS-MODEL (https://swissmodel.expasy.org) [39], respectively. UCSF Chimera was used for further modification of the structure [40].

2.5. Analysis of mRNA expression of HaGSTκ1

Real-time quantitative polymerase chain reaction (RT-qPCR) was

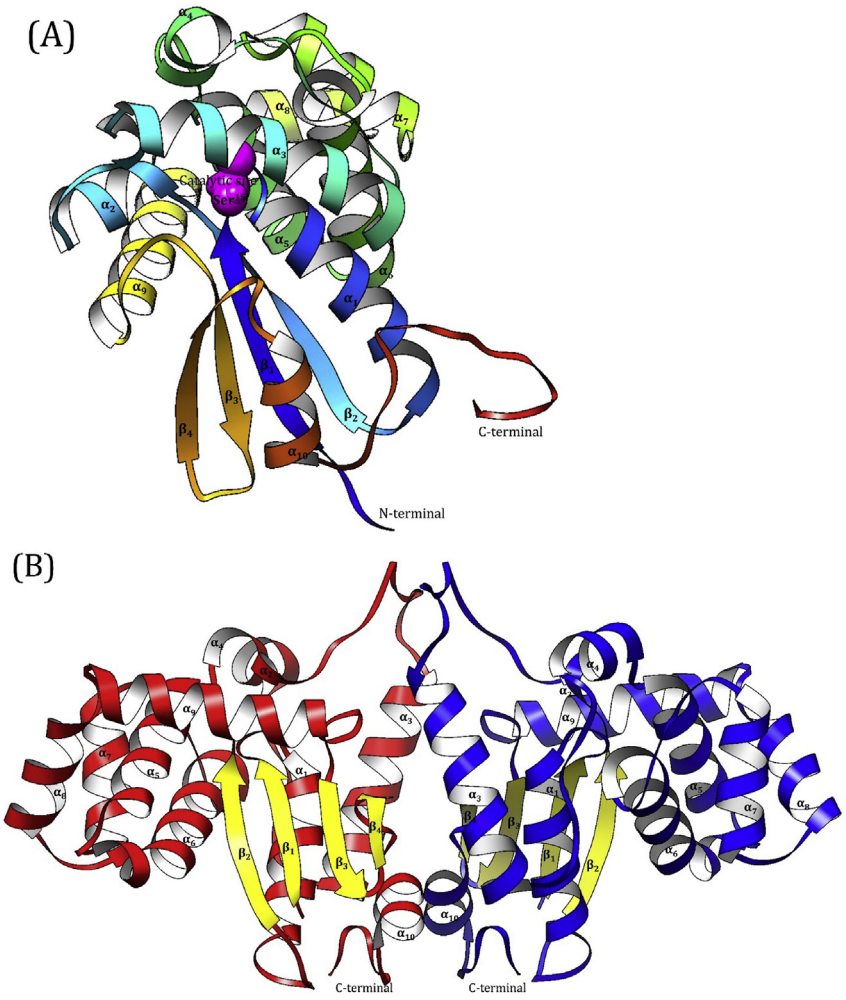

Fig. 1. A) Three-dimensional structure of HaGSTκ1. α-Helices and β-sheets are colored in different colors, and the catalytic "Ser" residue is displayed as a pink-colored sphere. B) HaGSTκ1 dimer with a butterfly-like shape is identical to the kappa class of GSTs. (For interpretation of the references to color in this figure legend, the reader is referred to the Web version of this article.)

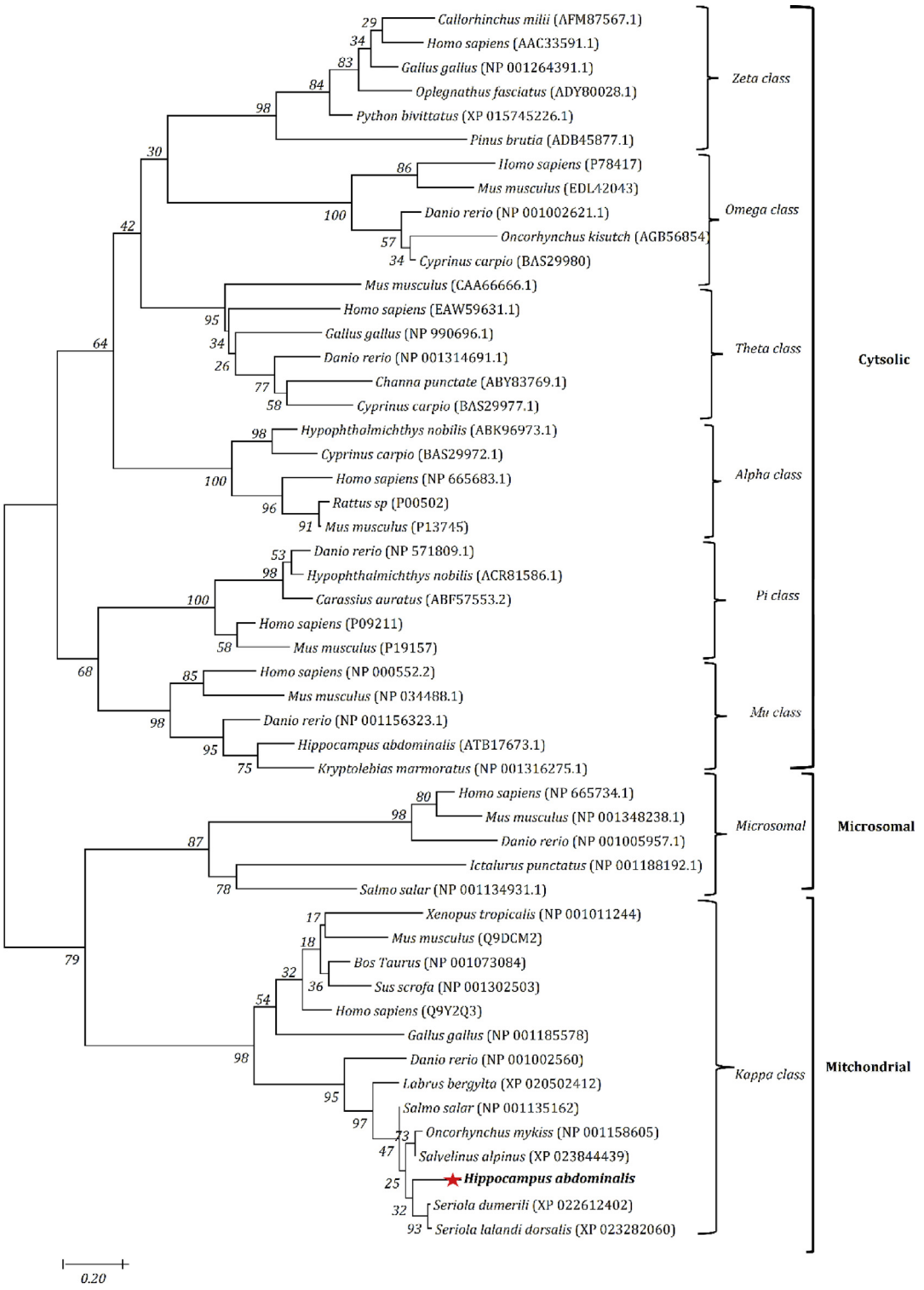

Fig. 2. Phylogenetic tree of HaGSTκ1 with other homologs from different classes of GSTs. MEGA 6.0 was used to construct the tree with 5,000 bootstrap values, and the values are mentioned on the nodes of branches. NCBI GenBank accession numbers are given with each species name.

performed to determine the tissue-specific and temporal mRNA expression profile of *HaGSTκ1* in unchallenged and immune challenged seahorses using Thermal Cycler Dice Real Time system III (TaKaRa, Japan). Seahorse 40S ribosomal protein S7 (Accession number: KP780177) was used as an internal control gene. The qPCR primers (Table 1) were designed according to Minimum Information for publication of Quantitative Real-Time PCR Experiment (MIQE) guidelines [41] using Primer Quest tool (https://sg.idtdna.com/site/account/login?returnurl=/Primerquest/Home/Index). The qPCR mixture was adjusted to 10 μL of final volume with 3 μL of cDNA template, 0.4 μL of each forward and reverse primer (10 pmol/μL) (Table 1), 1.2 μL nuclease-free water, and 5 μL of 2 × TaKaRa Ex Taq™ SYBR premix. The thermal profile of qPCR was proceeded for one cycle of initial denaturation at 95 °C for 30 s and 45 cycles at 95 °C for 5 s, 58 °C for 10 s, and 72 °C for 20 s, followed by a final cycle of 95 °C for 15 s, 60 °C for 30 s, and 95 °C for 15 s. The relative mRNA expression was calculated

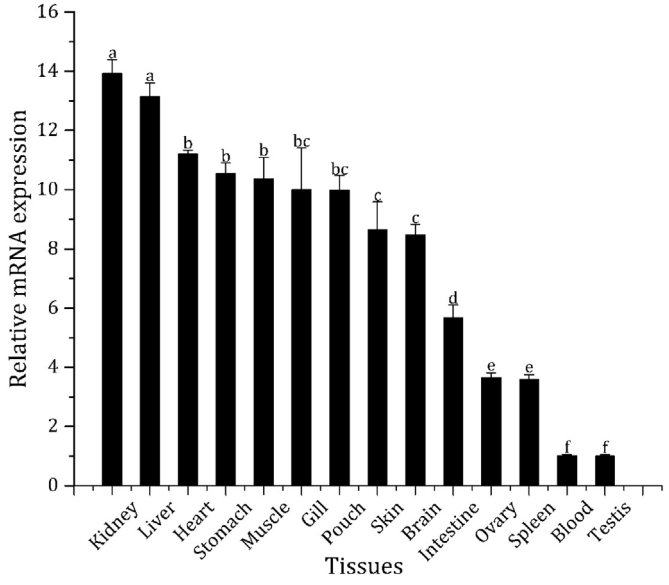

Fig. 3. Tissue-specific expression of HaGSTκ1 from unchallenged seahorse. The 40s ribosomal S7 protein was considered as an internal control gene, and Livak $2^{-\Delta\Delta Ct}$ method was used to calculate relative mRNA expression. The experiment was performed in triplicates (n = 3). Error bars represent standard deviations (SDs). The letters on the error bars indicate significant differences of fold values ($P < 0.05$) between each tissue.

with the Livak $2^{-\Delta\Delta CT}$ method [42]. The expression level of *HaGSTκ1* in the immune challenged seahorses was determined and compared with that in the PBS injected control seahorses at each time point. All reactions were performed in triplicates.

2.6. Cloning of HaGSTκ1 into pMAL-c5X

PCR was carried out using 5 μL of 10 × Ex Taq buffer, 4 μL of 2.5 mM dNTPs, 5 μL of liver cDNA template, 0.2 μL of Ex Taq DNA polymerase (5 units/μL) (TaKaRa, Japan), and 1 μL of each of forward and reverse primer (10 pmol/μL), and nuclease-free water (PCR grade) was used to make up the reaction volume to 50 μL. The cloning primers were designed with the *Not*I and *Eco*RI restriction sites (Table 1). The PCR thermal profile was adjusted to an initial denaturation at 95 °C for 5 min and 35 cycles of denaturation at 95 °C for 30 s, annealing at 56 °C for 30 s, elongation at 72 °C for 50 s, and a final extension at 72 °C for 7 min. The PCR product was run on a 1% agarose gel and purified using Accuprep™ gel purification kit (BIONEER, Korea). Plasmid extraction was performed for the vector pMAL-c5X (New England Biolabs Inc, USA) using the MG™ Plasmid SV miniprep kit (MG Med Inc, Korea). The purified pMAL-c5X and HaGSTκ1 PCR products were subjected to restriction digestion with relevant restriction enzymes and purified using AccuPrep® Gel Purification Kit (BIONEER, Korea). Products were ligated at 16 °C for 30 min and 4 °C overnight using Ligation Mix (TaKaRa, Japan). The ligated *HaGSTκ1*/pMAL-c5X construct was transformed into *Escherichia coli* DH5α competent cells, and the sequence was confirmed from Macrogen, Korea. The recombinant plasmids were transformed into *E. coli* BL21(DE3) competent cells (Novagen, Germany) for protein expression.

2.7. Overexpression and purification of recombinant HaGSTκ1 (rHaGSTκ1) fusion protein

A total of 500 mL of Luria Bertani (LB) rich medium was prepared with 1 g glucose and ampicillin (100 μg/mL). Transformed colonies were grown at 37 °C and 200 rpm, and 0.5 mM of isopropyl-β-thiogalactopyranoside (IPTG) (Promega, USA) was added to induce protein expression after the optical density (OD) reached 0.6 at 600 nm. The culture was further incubated at 20 °C and 200 rpm for 8 h. The induced cells were harvested at 1,200 × *g* and 4 °C for 20 min. The cells were resuspended in a column buffer (20 mM Tris-HCl, 200 mM sodium chloride [NaCl], pH 7.4) and stored at −20 °C. The cells were thawed in running cold water and incubated with 1 mg/mL lysozyme (Biosesang, Korea) for 30 min to facilitate cell lysis. Cells were sonicated, and the clear lysate was separated by centrifugation at 9,000 × *g* and 4 °C for 30 min. The supernatant was mixed with amylose resin (New England Biolabs, USA) and the recombinant fusion protein was purified using pMAL™ Protein Fusion and Purification System (New England Biolabs, USA) following the manufacturer's instruction. The concentrations of purified protein fractions were measured using Bradford assay [43], and the samples were separated on 12% sodium dodecyl sulfate polyacrylamide gel electrophoresis (SDS-PAGE) gels to determine the size and purity of the protein.

2.8. Functional characterizations of rHaGSTκ1

2.8.1. Enzyme assay for rHaGSTκ1

Enzymatic activity was separately evaluated using five different substrates, including 1 mM 1-chloro-2,4-dinitrobenzene (CDNB) (Sigma Aldrich, India), 1 mM 1,2-dichloro-4-nitrobenzene (DCNB) (Sigma Aldrich, Korea), 1 mM 4-nitrobenzyl chloride (4-NBC) (Sigma Aldrich, Korea), 1 mM 4-nitrophenethyl bromide (4-NPB) (Sigma Aldrich, Korea), and 1 mM ethacrynic acid (ECA) (Sigma Aldrich, Korea). The reaction was carried out in a 200 μL final volume containing 1 mM phosphate buffer at a suitable pH value (Table 2), 1 mM reduced GSH (Sigma Aldrich, Japan), 10 μg of rHaGSTκ1, and 1 mM of each substrate. The reaction was initiated after adding the substrate, followed by the measurement of the initial absorbance of the solution. Final absorbance was measured after a 5 min interval at suitable wavelengths (Table 2) [44] using a microplate reader (Thermo scientific Waltham, MA, USA). All assays were performed in triplicates, and the temperature was maintained at 25 °C.

2.8.2. Enzyme kinetics

The above procedure (2.8.1) was performed in the presence of varying concentrations of CDNB (0.25–4.0 mM) and a constant amount of reduced GSH (1 mM) as well as with varying concentrations of GSH (0.25–4.0 mM) and a constant amount of CDNB (1 mM) substrate to measure the Michaelis-Menten constant (K_m) and maximum reaction velocity (V_{max}) by the Lineweaver Burk plot.

2.8.3. Effect of pH, temperature, and inhibitors on the rHaGSTκ1 activity

To analyze the activity of rHaGSTκ1 at different pH values, a series of pH buffers (pH 3–10) were prepared. CDNB was used as a substrate and the experimental procedure reported in section 2.8.1 was followed. The activity against temperature was measured at a temperature range of 10 °C–60 °C. The inhibition of recombinant protein expression was measured against two inhibitors, Cibacron blue (CB) (Polyscience Inc, USA) and hematin porcine (Sigma Aldrich, Korea), at 0.001–100 μM and 0.001–10,000 μM concentration gradients, respectively.

2.9. Statistical analysis

All experiments were conducted in triplicate, and the results are expressed as mean relative expression ± standard deviation (SD). Tissue distribution results were statistically compared using one-way analysis of variance (ANOVA). Mean comparisons were conducted using Tukey's post-hoc pairwise comparison in the SPSS statistics 24 software (IBM Corporation, USA). For expression analysis of *HaGSTκ1* after immune challenge, results were statistically analyzed using one-way analysis of variance (ANOVA). Mean comparisons of the treatments were determined using Tukey's post-hoc pairwise comparison in the SPSS statistics 24 software (IBM Corporation, USA). Statistical significance was considered to be $p < 0.05$.

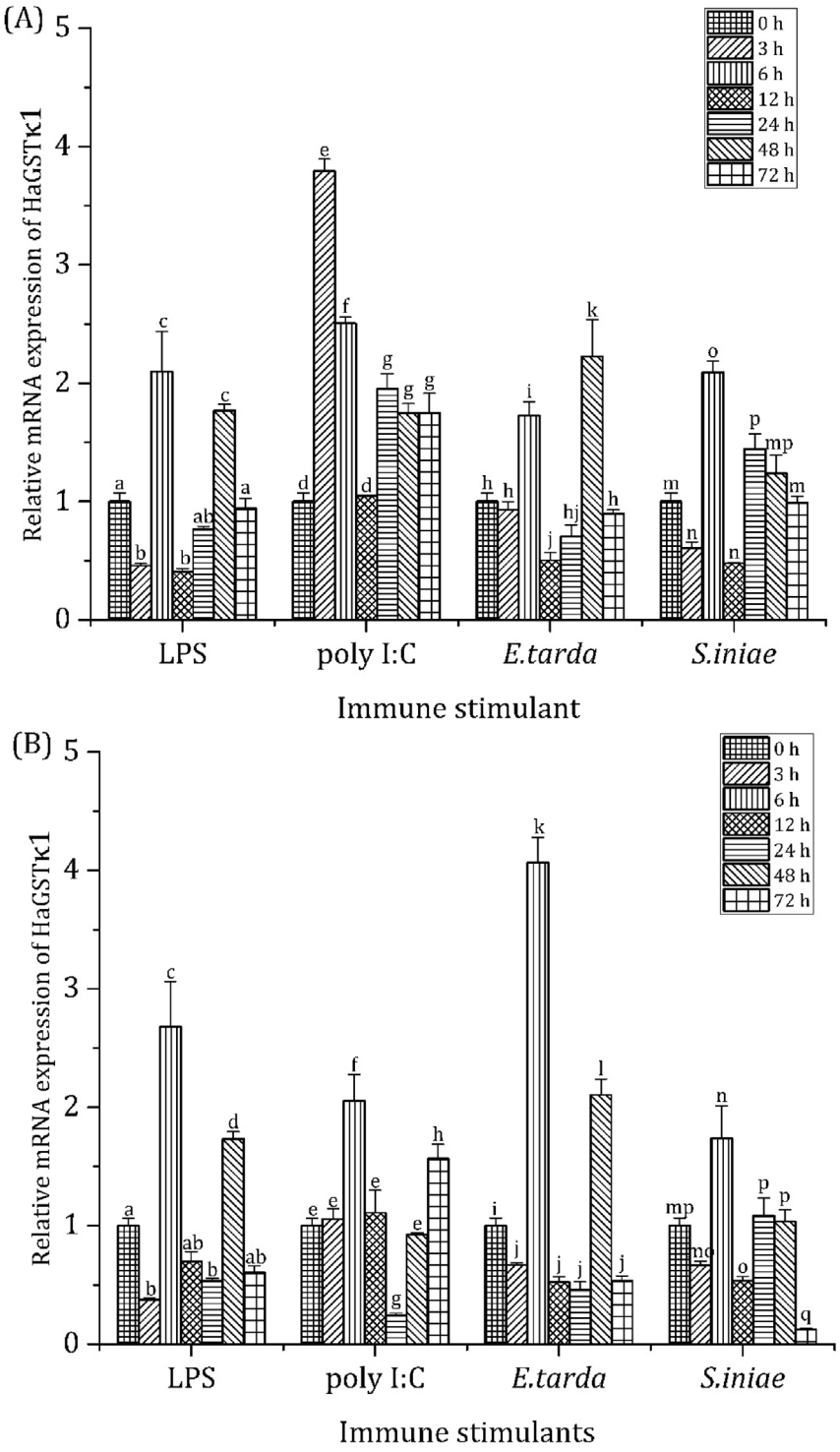

Fig. 4. A) Relative mRNA expression in the liver and B) blood tissues after LPS, poly I:C, *Edwardsiella tarda*, and *Streptococcus iniae* challenge at six different time points. The calculation was performed with Livak $2^{-\Delta\Delta Ct}$ method, and the values were normalized with those reported for the PBS-injected seahorses. The experiment was performed in triplicates (n = 3) and error bars represent the standard deviations (SDs). Statistical analysis was performed using one-way analysis of variance (ANOVA). Mean comparisons were determined by Tukey's post-hoc pairwise comparison to compare the treatments. Significant differences are compared to the blank (0 h) with $P < 0.05$.

3. Results

3.1. In silico analysis of HaGSTκ1

The identified *HaGSTκ1* (accession number: MK404305) comprised a 696 bp ORF encoding a polypeptide of 231 amino acid residues. The predicted molecular weight and theoretical isoelectric point (pI) values were 26.04 kDa and 8.28, respectively. Signal peptide and N-glycosylation sites were not detected according to the output results of SignalP 4.1 and NetNGlyc 1.0 Servers, respectively. NCBI conserved domain database, Motif Scan results, and SMART sequence analysis show that HaGSTκ1 belongs to the disulfide bond formation protein A (DsbA), GST kappa, and thioredoxin-like superfamilies with a thioredoxin domain held by an alpha helical domain and DsbA general fold within 6–213 amino acids. The GSH-binding sites were detected at Ser15-Tyr17, Asn52, Lys61, Phe183-Phe185, Phe200, and Ser202-Arg204 positions. The catalytic site was based at Ser15, and the dimer interfaces (polypeptide-binding sites) were located at Ser50, Asn52, Lys53, Val58, Asn60, Trp64, Asp68, Leu178, Met198, Phe200, Asp203, Arg204, and His210.

A 3D model of HaGSTκ1 was constructed using I-TASSER which provided the most matched structure as compared with the highest

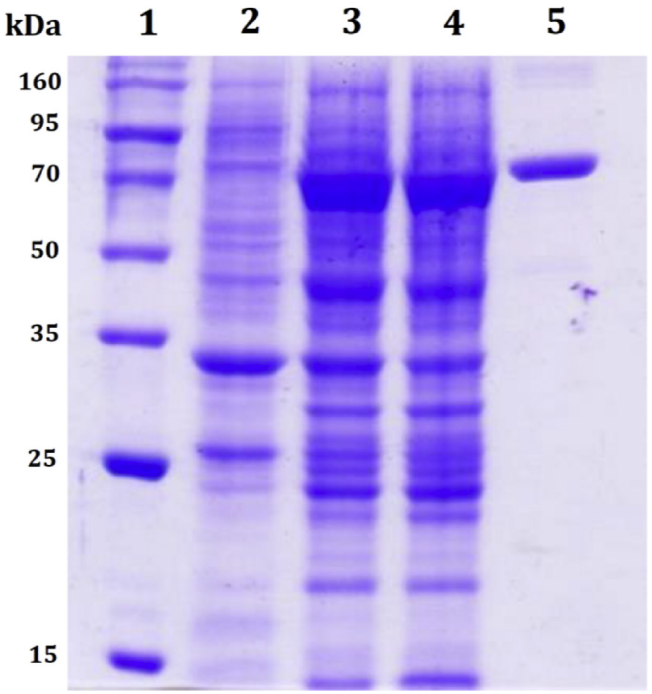

Fig. 5. SDS-PAGE analysis of purified rHaGSTκ1 as an MBP fusion protein. Lane 1: protein ladder, Lane 2: crude extract of un-induced *Escherichia coli* BL21 cells, Lane 3: crude extract of induced *Escherichia coli* BL21 cells, Lane 4: supernatant after centrifugation, Lane 5: purified HaGSTκ1 fusion protein.

significant structures of their library (Fig. 1) [38]. There were $\beta_1\alpha_1\beta_2$ and $\beta_3\beta_4\alpha_{10}$ motifs linked with eight α-helices. Four β-strands were located in anti-parallel directions. These α-helices and β-sheets contributed to the DsbA general fold (Fig. 1A). The dimer of HaGSTκ1 exhibited a butterfly-like structure in the SWISS-MODEL tool and showed 52.34% identity and 0.47% similarity with the crystal structure of human kappa glutathione transferase (Fig. 1B).

A maximum identity of 80.5% and similarity of 91.3% were observed in the pairwise sequence alignment with *Labrus bergylta* (Ballan wrasse). The identity and similarity ranged within 80.5–15.2% and 91.3–22.9%, respectively (Supplementary Table 1). The amino acid sequence alignment of HaGSTκ1 with other species reveals the high degree of conservation in GSH-binding sites and catalytic residues (Supplementary Fig. 1). The phylogenetic tree with 5,000 bootstrap steps showed the relationship with different GST classes. Of these, HaGSTκ1 belongs to the group of teleost GST kappa class (Fig. 2).

3.2. Tissue distribution of HaGSTκ1

The highest expression of *HaGSTκ1* was observed in the kidney and liver among the fourteen tissues analyzed. Heart, stomach, muscle gill, and pouch also showed high expression, while testis and blood showed the lowest expression (Fig. 3).

3.3. Expression profile of HaGSTκ1 mRNA after immune challenges

To investigate the immune responses of *HaGSTκ1* gene against immune stimulants, its relative expression levels were studied in the liver and blood samples after time-course challenge experiment (Fig. 4). The expression fold change values were analyzed compared to the expression of *HaGSTκ1* at the 0 h time point. The analysis of the temporal mRNA expression profile of *HaGSTκ1* in the liver showed that the transcript level was similar following LPS and *E. tarda* challenge. A significant upregulation in the expression pattern after LPS injection was stimulated at 6 h p.i. (2.1-fold) and 48 h p.i. (1.8-fold), which

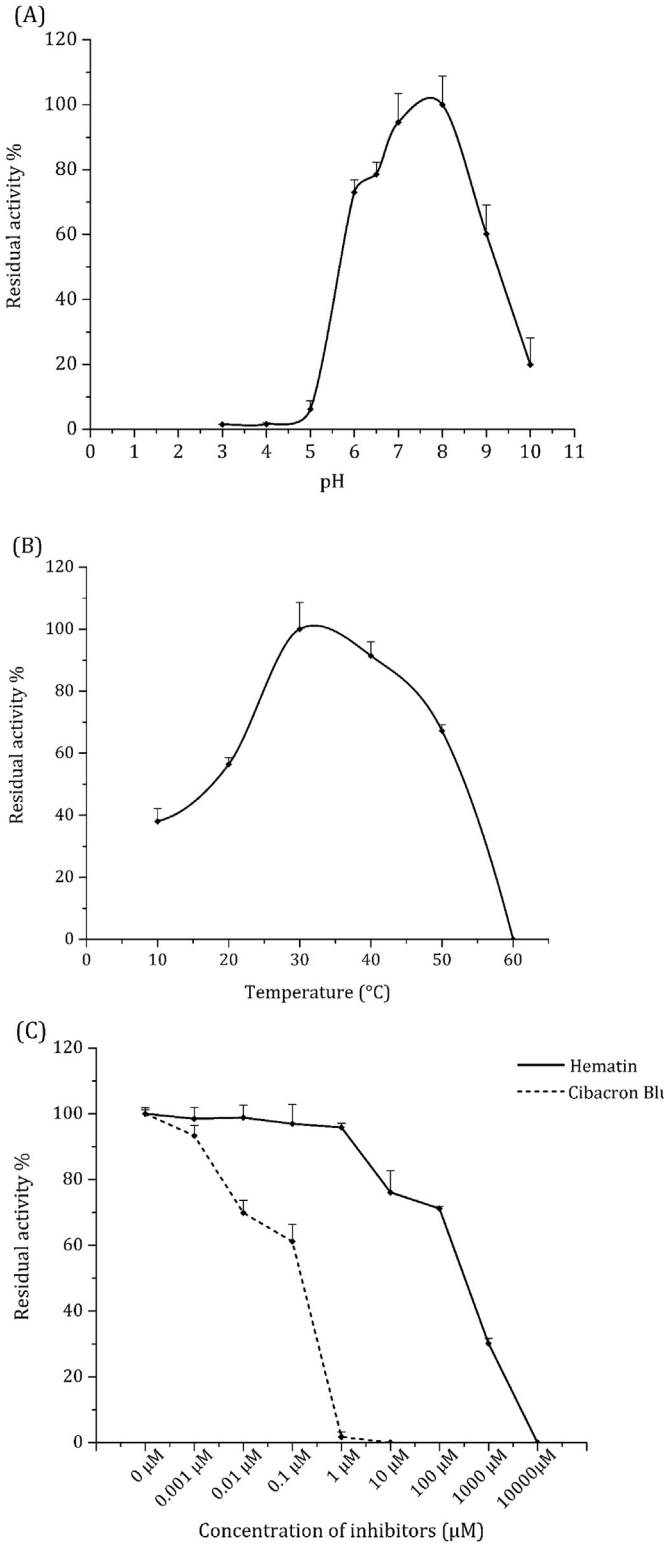

Fig. 6. Effects of A) pH, B) temperature, and C) inhibitors on the catalytic activity of HaGSTκ1. The experiment was performed in triplicates (n = 3). Error bars represent the standard deviations (SDs).

exhibited a similar pattern of upregulation as that for *E. tarda* injection at 6 h p.i. (1.7-fold) and 48 h p.i. (2.2-fold) ($P < 0.05$). The highest expression level (3.8-fold) was reported at 3 h p.i. after poly I:C injection, and the level gradually decreased until 12 h p.i. (1.0- fold) (Fig. 4A). The transcript level increased thereafter and showed a 2.0- to 1.7-fold increase from 24 h p.i. to 72 h p.i. (Fig. 4A). Upregulation in

Table 3
Catalytic activity, optimum pH and optimum temperature for previously studied GSTs.

GST enzyme	Species	Catalytic activity for fixed CDNB		Catalytic activity for fixed GSH		Optimum pH	Optimum Temperature
		K_m (mM)	V_{max} (μmol.min^{-1}mg^{-1})	K_m (mM)	V_{max} (μmol.min^{-1}mg^{-1})		
HaGSTκ1	Sea horse	0.513 ± 0.07	0.613 ± 0.08	0.276 ± 0.15	0.473 ± 0.07	8.0	30 °C
RfGSTρ [56]	Black rockfish	14.10 ± 0.25	11.28 ± 0.70	3.02 ± 0.08	3.40 ± 0.09	7.5	40 °C
AbGSTκ [19]	Disk abalone	2.95 ± 0.28	12.77 ± 0.29	3.81 ± 0.30	14.35 ± 0.30	8.0	35 °C
HaGSTρ [48]	Sea horse	0.78 ± 0.05	14.22 ± 1.02	0.59 ± 0.02	10.55 ± 0.36	10	37 °C
HaGSTμ [49]	Sea horse	4.21 ± 0.45	21.96 ± 2.20	0.63 ± 0.28	7.24 ± 1.55	8.0	40 °C
RpGSTσ [50]	Manila clam	–	–	–	–	7.5–8.5	30-35 °C
RpGSTθ [51]	Manila clam	–	–	–	–	5.5–6.5	35-40 °C

transcript level was observed at 6 h (2.1-fold) after *S. iniae* challenge (Fig. 4A) ($P < 0.05$).

Evaluation of the *HaGSTκ1* mRNA expression profile in the blood revealed that the pattern of transcription level was similar after LPS and *E. tarda* challenges. During the LPS challenge, the transcription level was significantly upregulated at 6 h p.i. and 48 h p.i. at 2.7-fold and 1.7-fold, respectively (Fig. 4B). A similar upregulation profile was detected at 6 h (4.0-fold) and 48 h (2.1-fold) for *E. tarda* injection (Fig. 4B) ($P < 0.05$). Furthermore, the expression of *HaGSTκ1* after poly I:C treatment was significantly upregulated at 6 h and 72 h respective to 0 h p.i. (Fig. 4B). The transcription of *HaGSTκ1* at 24 p.i. (0.2-fold) was downregulated in the challenged group compared with the unchallenged control. Moreover, the mRNA expression of *HaGSTκ1* showed considerable upregulation only at 6 h p.i (1.7-fold) following *S. iniae* injection (Fig. 4B).

3.4. Recombinant protein expression and purification

The rHaGSTκ1 protein was purified using amylose-affinity chromatography. The molecular mass identified from 12% SDS-PAGE was nearly 68 kDa (42.5 kDa maltose-binding protein [MBP] tag + 26 kDa rHaGSTκ1) (Fig. 5).

3.4.1. Specific activities of rHaGSTκ1 with different substrates and enzyme kinetics

The activity was detected using CDNB, ECA, 4-NBC, and 4-NPB substrates (Table 2). The maximum specific activity was observed with 4-NBC substrate (Table 2). However, no activity was reported for DCNB. The activity of MBP for negligible for each substrate. The K_m and V_{max} values for CDNB substrate were 0.513 ± 0.07 mM and 0.613 ± 0.08 μmol·min^{-1}·mg^{-1} respectively. For GSH, the K_m and V_{max} values were 0.276 ± 0.15 mM and 0.473 ± 0.07 μmol·min^{-1}·mg^{-1}, respectively.

3.4.2. Response of rHaGSTκ1 to varying pH, temperature, and inhibitors

The optimal enzymatic activity was observed at pH 8 (Fig. 6A) and a temperature of 30 °C (Fig. 6B) using CDNB as substrate. One hundred percent inhibition of rHaGSTκ1 activity toward CDNB was observed in the presence of CB and hematin at 100 μM and 10,000 μM concentrations, respectively (Fig. 6C). The IC_{50} value of HaGSTκ1 and CDNB reaction was 0.12 μM for CB and 398.11 μM for hematin (Fig. 6C).

4. Discussion

GSTs are the isoenzymes that mediate GSH-dependent cellular detoxification of xenobiotics, resulting in the production of less toxic soluble products for excretion. HaGSTκ1 is a mitochondrial enzyme that lacks signal peptide and N-glycosylation machinery. Hence, it is not synthesized through the secretory pathway and may not undergo glycosylation. According to the results of sequence characterization, HaGSTκ1 has a molecular weight of 26.04 kDa, similar to that of other GST enzymes (22–28 kDa) [19,45–47].

Results of 3D structure prediction showed that all the ten α-helices, coils, and four antiparallel β-sheets contribute to a DsbA general fold with thioredoxin domain. HaGSTκ1 showed a common arrangement belonging to the kappa class, including the βαβ ($\beta_1\alpha_1\beta_2$) motif and ββα ($\beta_3\beta_4\alpha_{10}$) motif linked by eight α-helices, as observed with human, rat, and mouse kappa classes [48]. In other classes, $\beta_1\alpha_1\beta_2$ and $\beta_3\beta_4\alpha_3$ motifs are connected with the α_2-helix in the N-terminal and C-terminal domains with a variable number of (4–7) α-helices [14]. For instance, GSTμ and GSTρ in seahorse (*Hippocampus abdominalis*) [49] and GSTσ [50] and GSTθ in Manila clamp (*Ruditapes philippinarum*) [51] showed the same arrangements. In kappa class, α-helices connect with the βαβ motif at the N-terminus and the ββα motif at the C-terminus [12]. Moreover, a special butterfly shape structure was observed for HaGSTκ1 dimer, consistent with the observations reported for other kappa classes of GSTs in the disk abalone [19], the giant prawn (*M. rosenbergii*) [18], and a camel (*Camelus dromedaries*) [46]. The 3D structure of HaGSTκ1 suggests that the protein has a domain arrangement similar to that of other kappa classes.

The GSH-binding sites, catalytic 'Ser' residue, and polypeptide-binding sites of HaGSTκ1 are conserved and showed different degrees of similarity with those from other organisms. The catalytic 'Ser' residue highly conserved between all other species activates GSH and catalyzes the formation of a hydrogen bond with sulfur in GSH via a water molecule [52]. In the C-terminus, the substrate-binding sites were not highly conserved, as the binding to different substrates may differ from species to species. HaGSTκ1 exhibited a close relationship with kappa classes of GSTs from marine fishes. Some organisms have more than one GST that belong to different classes, indicating specific GST genes for different types of xenobiotic detoxification [53].

Highest *HaGSTκ1* expression was observed in the kidney and liver as compared to other tissues. As per the previous results, GST kappa in mouse and rat showed high expression in the heart, kidney, and liver [54]. In humans, GST kappa showed high expression in the kidney and liver, similar to our results [55]. In the rock-fish (*Sebastes schlegelii*), GSTω, GSTρ, and GSTθ displayed prominent mRNA expression in the liver [56]. GSTμ and GSTρ in the big belly seahorse showed comparatively higher expression level in ovary and gills, respectively than in other tissues [49]. In Manila clam, the highest mRNA expression of GSTθ was observed in hemocytes and gills [51]. According to these results, the contribution of different GSTs for detoxification activity may vary in different tissues. The liver is considered as the major organ associated with detoxification of xenobiotics [57,58]. Most enzymes that participate in biotransformation are localized in the liver [59]. For instance, total cytochrome P-450 concentrations in the liver are higher than those in the kidney [60]. The kidney is the primary route for the end products of xenobiotics [60]. The enzymes in the kidney excrete soluble xenobiotics, drugs, and hormones through the renal excretory mechanism [61]. Therefore, the highest expression of HaGSTκ1 in the liver and kidney tissues is suggestive of their possible involvement in the xenobiotic detoxification process.

GSTs are multifunctional enzymes [62] that show an immune response against bacterial [63] and viral infections [64]. Previous studies

have revealed a considerable upregulation in the expression of several GST types during an immune challenge in seahorse (*Hippocampus abdominalis*) [49], black rockfish (*Sebastes schlegelii*) [56], disk abalone (*Haliotis discus discus*) [19], and the Manila clam (*Ruditapes philippinarum*) [50,51,65]. Blood tissue is responsible for the circulation of gases, nutrients, and metabolites to target organs in vertebrates. White blood cells participate in the innate and adaptive immunity by expressing immune-related genes [66]. Previous studies have revealed the immune function of red blood cells [67,68]. The liver is considered as a mediator of the systemic and local innate immune responses [69]. Therefore, blood and liver were selected as the target tissues for the analysis of *HaGSTκ1* expression following immune stimulation. To examine the expression level of *HaGSTκ1*, the seahorses were challenged with LPS, poly I:C, *E. tarda*, and *S. iniae*. LPS is an endotoxin from the outer membranes of gram-negative bacteria [70]. In this experiment, the mRNA expression profiles of *HaGSTκ1* following LPS challenge were similar in the liver and blood samples, as observed for GSTμ in Manila clam hemocytes [65]. *E. tarda* is a gram-negative enterobacterium and the causative agent of severe infections in a variety of fish species [71]. Symptoms may be observed in internal organs such as the liver, spleen, and kidney [72]. The expression pattern of HaGSTκ1 upon *E. tarda* infection was quite similar to that observed for GSTσ in Manila clam following *Vibrio tapetis* (a gram-negative bacterium) infection in hemocytes [65]. *S. iniae* causes high mortality and morbidity of fishes and is also associated with human diseases [73,74]. However, we failed to observe any significant upregulation in the expression of *HaGSTκ1* in blood following *S. iniae* challenge. However, a minor upregulation in *HaGSTκ1* expression was detected in the liver. For poly I:C stimulation, *HaGSTκ1* expression was highly upregulated in the liver at an early stage, similar to that observed for GSTω in the blood cells of rockfish [56].

Phagocyte respiratory burst is a response evolved from the innate immune system of fishes following pathogenic infection [75]. After microbial infection, the number of macrophages increased in the early phase that resulted in the phagocytosis of the invading pathogenic bacteria by neutrophils within 24–48 h [76]. Complement receptor 3 (CR3) in phagocytic cells indirectly interacts with LPS on the outer membrane of gram-negative bacteria [77]. As a result, the production of reactive oxygen species (ROS) increased [78] to eradicate the invading pathogen. Overproduction of ROS results in the generation of oxidative stress and inhibition of the activities of biological molecules [79]. To maintain cellular homeostasis, ROS level is maintained by several antioxidant enzymes, including GST. GST expression upregulation was observed in response to organic hydroperoxides, lipid peroxidation products, and endotoxic bacterial components generated following bacterial challenge [80]. Similar *HaGSTκ1* expression pattern was observed in seahorse blood and liver samples after LPS and bacterial administration. Previous studies have described the upregulation in the expression of GSTs in response to ROS in mammals and plants [81–83]. In bumblebee, GST sigma expression was shown to be induced after the oxidative burst from hydrogen peroxide [84]. Moreover, GST may be involved in the detoxification of toxic lipid peroxidation products produced by the bacteria in the midgut of *Galleria mellonella* [80]. The early phase (6 h) *HaGSTκ1* expression upregulation may be associated with the production of excessive ROS through the phagocytosis of bacteria by macrophages. The activity of macrophages produces proinflammatory cytokines such as interleukin (IL)-1β, IL-6, and tumor necrosis factor (TNF)-α [85–87]. A previous study proved that interleukin-1β expression was shown to reduce the alpha GST level in human intestinal epithelial cells [88]. Another study showed the downregulation of the expression of GST subunits by IL-1β in rat hepatocytes [89]. The downregulation in *HaGSTκ1* expression after bacterial challenge may be related to the production of IL-1β from macrophages. To understand the mechanism underlying *HaGSTκ1* action against ROS, further experiments are warranted to evaluate GST expression following the pathogenic attack. Virus infections also generate ROS from phagocytes [90]. *HaGSTκ1* mRNA expression was prominently elevated in the liver and blood in the early phase (3 and 6 h, respectively) following poly I:C challenge. This observation may be attributed to the regulation of the redox state of seahorse against respiratory burst from ROS metabolites during phagocytosis. Altogether, the results revealed the involvement of HaGSTκ1 in the immunity of seahorse under pathogenic infection.

The specific activity of rHaGSTκ1 was measured with five different aryl halides; the highest activity was reported for 4-NPB (Table 2). Other studies with GSTμ in Manila clam [65] and seahorse [49] revealed the highest specific activities of the protein for the 4-NPB substrate. Disk abalone GSTκ [19], seahorse GSTμ, and GSTρ [49] showed no activity for DCNB substrate, consistent with the results of the present study. Abalone GSTκ showed activity only toward CDNB substrate [19]. Furthermore, most GSTs showed maximum activity toward CDNB. GSTσ from Manila clam [50], GSRρ and GSTθ from black rock-fish [56], and the first kappa class of GST from rat showed the highest activities for CDNB substrate [17]. These results suggest that the same class of GSTs within different organisms may exhibit different affinities for substrates. Furthermore, the affinity for substrates differed from one class of GST to another class within the same organism. Therefore, GSTs may act in different ways to metabolize the xenobiotics produced under several environmental conditions.

CDNB substrate was used to investigate the kinetic parameters and optimum conditions for HaGSTκ1 activity. CDNB is considered as a universal substrate for most GST classes [15]. To determine enzyme kinetics, the K_m and V_{max} values were calculated at different CDNB substrate and GSH concentrations. The K_m values were nearly similar to the results of GSTρ in seahorse [49] (Table 3) and are indicative of the high affinity of HaGSTκ1 for CDNB as compared with other GSTs. The enzyme is saturated at low concentrations of substrate.

The optimum pH and temperature for rHaGSTκ1 were 8 and 30 °C, respectively. This pH value is closely related to the optimum pH of disk abalone GSTκ [19], seahorse GSTμ [49], and GSTρ of black rockfish [56] (Table 3). The pH value for the seahorse aquarium was recommended to be maintained at approximately pH 8 [91]; most of fish aquariums use 6.5–9 pH for fish farming. The solubility and toxicity of chemicals and heavy metals in the water can vary with the pH value of water [92]. Interestingly, the highest activity of rHaGSTκ1 was also exhibited at pH 8 which is the preferable pH value for seahorse growth. Furthermore, considerable activity was detected within the 6–9 pH range indicating that rHaGSTκ1 may be able to detoxify toxic compounds under different environmental conditions with different pH values.

The optimum temperature for GSTs in previous studies ranged between 30 °C and 40 °C (Table 3). These values may vary among animals and GST classes. The activity of rHaGSTκ1 was displayed in a wide range of temperatures indicating it may be stable under thermal stress conditions. Moreover, optimum activity may be dependent upon species and substrates. In general, GSTs show activity in a broad range of pH and temperature to help the organisms adjust to their environments.

Inhibition assay for rHaGSTκ1 activity was performed using CB and hematin inhibitors. CB has been used as the most effective inhibitor of several GSTs [93]. In our study, rHaGSTκ1 activity was rapidly inhibited by CB than hematin. A previous study with the kappa class of GST from abalone showed an IC_{50} value of 0.05 ± 0.01 μM for CB, indicative of the effective inhibition of rHaGSTκ1 activity [19]. Moreover, the IC_{50} values of hematin for rockfish GSTω, GSTρ, and GSTθ were lower than those of CB. For GSTμ in Manila clamp, the IC_{50} values were 0.65 μM and 9 μM for CB and hematin, respectively [65]. The inhibition effects on GST activity with these two inhibitors differed between species, types of GSTs, and substrates.

In conclusion, HaGSTκ1 was identified from the cDNA library and cloned into the pMAL-c5X vector. The recombinant protein was purified, and its enzymatic activity was assessed using different substrates. The optimum temperature and pH, inhibition activity, and enzyme

kinetics of the enzyme were determined with CDNB substrate. As the key organs involved in detoxification, the kidney and liver tissues showed the highest expression of *HaGSTκ1*. The relative mRNA expression of *HaGSTκ1* in the liver and blood tissue following challenge with LPS, poly I:C, *E. tarda*, and *S. iniae* revealed the immune response against the pathogenic attack. Altogether, these data suggest that HaGSTκ1 is another important GST that belongs to the mitochondrial kappa class with several variations from other GSTs and may play a critical role in the detoxification process and immunity of the animal.

Acknowledgments

This research was a part of the project titled 'Fish Vaccine Research Center' funded by the Ministry of Oceans and Fisheries, Korea and supported by Basic Science Research Program through the National Research Foundation of Korea (NRF) funded by the Ministry of Education (2019R1A6A1A03033553).

Appendix A. Supplementary data

Supplementary data to this article can be found online at https://doi.org/10.1016/j.fsi.2019.06.010.

References

[1] Y. Kanaoka, H. Ago, E. Inagaki, T. Nanayama, M. Miyano, R. Kikuno, Y. Fujii, N. Eguchi, H. Toh, Y. Urade, O. Hayaishi, Cloning and crystal structure of hematopoietic prostaglandin D synthase, Cell 90 (1997) 1085–1095, https://doi.org/10.1016/S0092-8674(00)80374-8.

[2] E. Petit, X. Michelet, C. Rauch, J. Bertrand-Michel, F. Tercé, R. Legouis, F. Morel, Glutathione transferases kappa 1 and kappa 2 localize in peroxisomes and mitochondria, respectively, and are involved in lipid metabolism and respiration in Caenorhabditis elegans, FEBS J. 276 (2009) 5030–5040, https://doi.org/10.1111/j.1742-4658.2009.07200.x.

[3] A. Dulhunty, P. Gage, S. Curtis, G. Chelvanayagam, P. Board, The glutathione transferase structural family includes a nuclear chloride channel and a ryanodine receptor calcium release channel modulator, J. Biol. Chem. 276 (2001) 3319–3323, https://doi.org/10.1074/jbc.M007874200.

[4] S.G. Cho, Y.H. Lee, H.S. Park, K. Ryoo, K.W. Kang, J. Park, S.J. Eom, M.J. Kim, T.S. Chang, S.Y. Choi, J. Shim, Y. Kim, M.S. Dong, M.J. Lee, S.G. Kim, H. Ichijo, E.J. Choi, Glutathione S-transferase mu modulates the stress-activated signals by suppressing apoptosis signal-regulating kinase 1, J. Biol. Chem. 276 (2001) 12749–12755, https://doi.org/10.1074/jbc.M005561200.

[5] C. Amantis, A. Queens, Chapter 7, English, (1927), https://doi.org/10.1016/B978-0-88415-758-8.50008-9.

[6] J.A. Timbrell, T.C. Marrs, Biotransformation of xenobiotics, Gen. Appl. Toxicol. (2009), https://doi.org/10.1002/9780470744307.gat004.

[7] D.J. Liska, The detoxification enzyme systems, Altern. Med. Rev. 3 (1998) 187–198 http://www.altmedrev.com/publications/3/3/187.pdf.

[8] R.M.E. Vos, P.J. Van Bladeren, Glutathione S-transferases in relation to their role in the biotransformation of xenobiotics, Chem. Biol. Interact. 75 (1990) 241–265, https://doi.org/10.1016/0009-2797(90)90069-Y.

[9] A. Worku Muleta, Glutathione Transferases as Detoxification Agents: Structural and Functional Studies, (2016).

[10] H. Wen, H. Yang, Y.J. An, J.M. Kim, D.H. Lee, X. Jin, S. Park, K.-J. Min, S. Park, Enhanced phase II detoxification contributes to beneficial effects of dietary restriction as revealed by multi-platform metabolomics studies, Mol. Cell. Proteom. 12 (2013) 575–586, https://doi.org/10.1074/mcp.M112.021352.

[11] H.L. Liston, J.S. Markowitz, C.L. DeVane, Drug glucuronidation in clinical psychopharmacology, J. Clin. Psychopharmacol. 21 (2001) 500–515, https://doi.org/10.1097/00004714-200110000-00008.

[12] J.D. Hayes, J.U. Flanagan, I.R. Jowsey, Glutathione transferases, Annu. Rev. Pharmacol. Toxicol. 45 (2005) 51–88, https://doi.org/10.1146/annurev.pharmtox.45.120403.095857.

[13] B. Mannervik, U.H. Danielson, 283 Glutathione Transferases - Structure and Catalytic Activity, (1988), p. 23.

[14] C. Frova, Glutathione transferases in the genomics era: new insights and perspectives, Biomol. Eng. 23 (2006) 149–169, https://doi.org/10.1016/j.bioeng.2006.05.020.

[15] D. SHEEHAN, G. MEADE, V.M. FOLEY, C.A. DOWD, Structure, function and evolution of glutathione transferases: implications for classification of non-mammalian members of an ancient enzyme superfamily, Biochem. J. 360 (2001) 1–16, https://doi.org/10.1042/bj3600001.

[16] T. Pandey, S.K. Singh, G. Chhetri, T. Tripathi, A.K. Singh, Characterization of a highly pH stable Chi-class glutathione S-transferase from Synechocystis PCC 6803, PLoS One 10 (2015) 1–15, https://doi.org/10.1371/journal.pone.0126811.

[17] J.M. Harris, D.J. Meyer, B. Coles, B. Ketterer, A novel glutathione transferase (13-13) isolated from the matrix of rat liver mitochondria having structural similarity to class theta enzymes, Biochem. J. 278 (1991) 137–141, https://doi.org/10.1042/bj2780137.

[18] M.K. Chaurasia, G. Ravichandran, F. Nizam, M.V. Arasu, N.A. Al-Dhabi, A. Arshad, R. Harikrishnan, J. Arockiaraj, In-silico analysis and mRNA modulation of detoxification enzymes GST delta and kappa against various biotic and abiotic oxidative stressors, Fish Shellfish Immunol. 54 (2016) 353–363, https://doi.org/10.1016/j.fsi.2016.04.031.

[19] W.M.G. Sandamalika, T.T. Priyathilaka, D.S. Liyanage, S. Lee, H.K. Lim, J. Lee, Molecular characterization of kappa class glutathione S-transferase from the disk abalone (Haliotis discus discus) and changes in expression following immune and stress challenges, Fish Shellfish Immunol. 77 (2018) 252–263, https://doi.org/10.1016/j.fsi.2018.03.058.

[20] L. Hao, P. Xie, J. Fu, G. Li, Q. Xiong, H. Li, The effect of cyanobacterial crude extract on the transcription of GST mu, GST kappa and GST rho in different organs of goldfish (Carassius auratus), Aquat. Toxicol. 90 (2008) 1–7, https://doi.org/10.1016/j.aquatox.2008.07.006.

[21] R. Pollom, Hippocampus Abdomimalis, The IUCN Red List of Threatened Species 2017, 2017.

[22] K. Kumaravel, S. Ravichandran, R. Balasubramanian, K.S. Subramanian, B.A. Bhat, Antimicrobial effect of five seahorse species from Indian coast, Br. J. Pharmacol. Toxicol. 1 (2010) 62–66.

[23] A.C.J. Vincent, R.S. Clifton-Hadley, Parasitic a case, J. Wildl. Dis. 25 (1989) 404–406.

[24] C.H. Chang, N.H. Jang-Liaw, Y.S. Lin, Y.C. Fang, K.T. Shao, Authenticating the use of dried seahorses in the traditional Chinese medicine market in Taiwan using molecular forensics, J. Food Drug Anal. 21 (2013) 310–316, https://doi.org/10.1016/jjfda.2013.07.010.

[25] R. Johansen Needham, J.R, D.J. Colquhoun, Guidelines for health and welfare monitoring of fish used in research, Lab. Anim. 40 (2006) 323–340.

[26] M. Oh, N. Umasuthan, D.A.S. Elvitigala, Q. Wan, E. Jo, J. Ko, G.E. Noh, S. Shin, S. Rho, J. Lee, First comparative characterization of three distinct ferritin subunits from a teleost: evidence for immune-responsive mRNA expression and iron depriving activity of seahorse (Hippocampus abdominalis) ferritins, Fish Shellfish Immunol. 49 (2016) 450–460, https://doi.org/10.1016/j.fsi.2015.12.039.

[27] S.F. Altschul, W. Gish, W. Miller, E.W. Myers, D.J. Lipman, Basic local alignment search tool, J. Mol. Biol. 215 (1990) 403–410, https://doi.org/10.1016/S0022-2836(05)80360-2.

[28] K. Okonechnikov, O. Golosova, M. Fursov, A. Varlamov, Y. Vaskin, I. Efremov, O.G. German Grehov, D. Kandrov, K. Rasputin, M. Syabro, T. Tleukenov, U.G.E.N.E. Unipro, A unified bioinformatics toolkit, Bioinformatics 28 (2012) 1166–1167, https://doi.org/10.1093/bioinformatics/bts091.

[29] M.R. Wilkins, E. Gasteiger, A. Bairoch, J. Sanchez, K.L. Williams, R.D. Appel, D.F. Hochstrasser, Protein identification and analysis tools in the ExPASy server, Methods Mol. Biol. 112 (2005) 531–552, https://doi.org/10.1385/1592595847.

[30] A. Marchler-Bauer, Y. Bo, L. Han, J. He, C.J. Lanczycki, S. Lu, F. Chitsaz, M.K. Derbyshire, R.C. Geer, N.R. Gonzales, M. Gwadz, D.I. Hurwitz, F. Lu, G.H. Marchler, J.S. Song, N. Thanki, Z. Wang, R.A. Yamashita, D. Zhang, C. Zheng, L.Y. Geer, S.H. Bryant, CDD/SPARCLE: functional classification of proteins via subfamily domain architectures, Nucleic Acids Res. 45 (2017) D200–D203, https://doi.org/10.1093/nar/gkw1129.

[31] C.J.A. Sigrist, E. De Castro, L. Cerutti, B.A. Cuche, N. Hulo, A. Bridge, L. Bougueleret, I. Xenarios, New and continuing developments at PROSITE, Nucleic Acids Res. 41 (2013) 344–347, https://doi.org/10.1093/nar/gks1067.

[32] T.N. Petersen, S. Brunak, G. Von Heijne, H. Nielsen, SignalP 4.0: discriminating signal peptides from transmembrane regions, Nat. Methods 8 (2011) 785–786, https://doi.org/10.1038/nmeth.1701.

[33] S.E. Hamby, J.D. Hirst, Prediction of glycosylation sites using random forests, BMC Bioinf. 9 (2008) 1, https://doi.org/10.1186/1471-2105-9-500.

[34] P. Rice, L. Longden, A. Bleasby, EMBOSS: the european molecular biology open software suite, Trends Genet. 16 (2000) 276–277, https://doi.org/10.1016/S0168-9525(00)02024-2.

[35] M.A. Larkin, G. Blackshields, N.P. Brown, R. Chenna, P.A. Mcgettigan, H. McWilliam, F. Valentin, I.M. Wallace, A. Wilm, R. Lopez, J.D. Thompson, T.J. Gibson, D.G. Higgins, Clustal W and clustal X version 2.0, Bioinformatics 23 (2007) 2947–2948, https://doi.org/10.1093/bioinformatics/btm404.

[36] W.L. Perry, JavaScript DNA Translator: DNA-aligned protein translations, Biotechniques 33 (2002) 1318–1320.

[37] K. Tamura, G. Stecher, D. Peterson, A. Filipski, S. Kumar, MEGA6: molecular evolutionary genetics analysis version 6.0, Mol. Biol. Evol. 30 (2013) 2725–2729, https://doi.org/10.1093/molbev/mst197.

[38] J. Yang, Y. Zhang, I-TASSER server: new development for protein structure and function predictions, Nucleic Acids Res. 43 (2015), https://doi.org/10.1093/nar/gkv342 W174–W181.

[39] A. Waterhouse, M. Bertoni, S. Bienert, G. Studer, G. Tauriello, R. Gumienny, F.T. Heer, T.A.P. De Beer, C. Rempfer, L. Bordoli, R. Lepore, T. Schwede, SWISS-MODEL: homology modelling of protein structures and complexes, Nucleic Acids Res. 46 (2018), https://doi.org/10.1093/nar/gky427 W296–W303.

[40] E.F. Pettersen, T.D. Goddard, C.C. Huang, G.S. Couch, D.M. Greenblatt, E.C. Meng, T.E. Ferrin, UCSF Chimera–a visualization system for exploratory research and analysis, J. Comput. Chem. 25 (2004) 1605–1612, https://doi.org/10.1002/jcc.20084.

[41] S.A. Bustin, V. Benes, J.A. Garson, J. Hellemans, J. Huggett, M. Kubista, R. Mueller, T. Nolan, M.W. Pfaffl, G.L. Shipley, J. Vandesompele, C.T. Wittwer, The MIQE guidelines: minimum information for publication of quantitative real-time PCR experiments, Clin. Chem. 55 (2009) 611–622, https://doi.org/10.1373/clinchem.2008.112797.

[42] K.J. Livak, T.D. Schmittgen, Analysis of relative gene expression data using real-time quantitative PCR and the 2-ΔΔCT method, Methods 25 (2001) 402–408, https://doi.org/10.1006/meth.2001.1262.

[43] M.M. Bradford, A rapid and sensitive method for the quantitation of microgram quantities of protein utilizing the principle of protein-dye binding, Anal. Biochem. 72 (1976) 248–254, https://doi.org/10.1016/0003-2697(76)90527-3.

[44] W.H. Habig, M.J. Pabst, W.B. Jakoby, Glutathione S-transferases, The first enzymatic step in mercapturic acid formation, J. Biol. Chem. 249 (1974) 7130–7139.

[45] T. Konishi, K. Kato, T. Araki, K. Shiraki, M. Takagi, Y. Tamaru, A new class of glutathione S-transferase from the hepatopancreas of the red sea bream Pagrus major, Biochem. J. 388 (2005) 299–307, https://doi.org/10.1042/BJ20041578.

[46] F.S. Ataya, A.A. Al-Jafari, M.S. Daoud, A.A. Al-Hazzani, A.I. Shehata, H.M. Saeed, D. Fouad, Genomics, phylogeny and in silico analysis of mitochondrial glutathione S-transferase-kappa from the camel Camelus dromedarius, Res. Vet. Sci. 97 (2014) 46–54, https://doi.org/10.1016/j.rvsc.2014.04.004.

[47] Y. Shao, Z. Lv, C. Li, W. Zhang, X. Duan, Q. Qiu, C. Jin, X. Zhao, Molecular cloning and functional characterization of theta class glutathione S-transferase from Apostichopus japonicus, Fish Shellfish Immunol. 63 (2017) 31–39, https://doi.org/10.1016/j.fsi.2017.02.004.

[48] J. Li, Z. Xia, J. Ding, Thioredoxin-like domain of human κ class glutathione transferase reveals sequence homology and structure similarity to the θ class enzyme, Protein Sci. 14 (2005) 2361–2369, https://doi.org/10.1110/ps.051463905.

[49] M.D.N. Tharuka, S.D.N.K. Bathige, J. Lee, Molecular cloning, biochemical characterization, and expression analysis of two glutathione S-transferase paralogs from the big-belly seahorse (Hippocampus abdominalis), Comp. Biochem. Physiol. B Biochem. Mol. Biol. 214 (2017) 1–11, https://doi.org/10.1016/j.cbpb.2017.08.005.

[50] N. Umasuthan, K. Saranya Revathy, Y. Lee, I. Whang, C.Y. Choi, J. Lee, A novel molluscan sigma-like glutathione S-transferase from Manila clam, Ruditapes philippinarum: cloning, characterization and transcriptional profiling, Comp. Biochem. Physiol. C Toxicol. Pharmacol. 155 (2012) 539–550, https://doi.org/10.1016/j.cbpc.2012.01.001.

[51] K. Saranya Revathy, N. Umasuthan, Y. Lee, C.Y. Choi, I. Whang, J. Lee, First molluscan theta-class Glutathione S-Transferase: identification, cloning, characterization and transcriptional analysis post immune challenges, Comp. Biochem. Physiol. - B Biochem. Mol. Biol. 162 (2012) 10–23, https://doi.org/10.1016/j.cbpb.2012.02.004.

[52] P.G. Board, M. Coggan, M.C. Wilce, M.W. Parker, Evidence for an essential serine residue in the active site of the Theta class glutathione transferases, Biochem. J. 311 (Pt 1) (1995) 247–250, https://doi.org/10.1042/bj3110247.

[53] B. Mannervik, Y.C. Awasthi, P.G. Broard, J.D. Hayes, C. Di Ilio, B. Ketterer, L. Listowsky, R. Morgenstern, M. Muramatsu, W.R. Pearson, Nomenclature for human glutathione transferases, Biochem. J. 282 (1992) 305–306, https://doi.org/10.1111/j.1399-0039.2011.01760.x.

[54] I.R. Jowsey, R.E. Thomson, T.C. Orton, C.R. Elcombe, J.D. Hayes, Biochemical and genetic characterization of a murine class Kappa glutathione S-transferase, Biochem. J. 373 (2003) 559–569, https://doi.org/10.1042/BJ20030415.

[55] F. Morel, C. Rauch, E. Petit, A. Piton, N. Theret, B. Coles, A. Guillouzo, Gene and protein characterization of the human glutathione *S* -transferase kappa and evidence for a peroxisomal localization, J. Biol. Chem. 279 (2004) 16246–16253, https://doi.org/10.1074/jbc.M313357200.

[56] J.D.H.E. Jayasinghe, S.D.N.K. Bathige, B.H. Nam, J.K. Noh, J. Lee, Comprehensive characterization of three glutathione S-transferase family proteins from black rockfish (Sebastes schlegelii), Comp. Biochem. Physiol. C Toxicol. Pharmacol. 189 (2016) 31–43, https://doi.org/10.1016/j.cbpc.2016.07.003.

[57] D.J. Waxman, C. Attisano, F.P. Guengerich, D.P. Lapenson, Human liver microsomal steroid metabolism: identification of the major microsomal steroid hormone 6 beta-hydroxylase cytochrome P-450 enzyme, Arch. Biochem. Biophys. 263 (1988) 424–436.

[58] C.D. Klaassen, C. Asarett, D. Oull, S Toxicology, (2008), https://doi.org/10.1036/0071470514.

[59] M.J. Meredith, D.J. Reed, Status of the mitochondrial pool of glutathione in the isolated hepatocyte, J. Biol. Chem. 257 (1982) 3747–3753.

[60] E.A. Lock, C.J. Reed, Xenobiotic metabolizing enzymes of the kidney, Toxicol. Pathol. 26 (1) (1998) 18–25 https://doi.org/10.1177/019262339802600102.

[61] J.W. Lohr, G.R. Willsky, M. a Acara, Renal drug metabolism, Pharmacol. Rev. 50 (1998) 107–141.

[62] K. Scott, M.J. Leaver, S.G. George, Regulation of hepatic glutathione S-transferase expression in flounder, Mar. Environ. Res. 34 (1992) 233–236 wos:A1992KB00500041.

[63] C. Wang, J. Zhao, C. Mu, Q. Wang, H. Wu, C. Wang, CDNA cloning and mRNA expression of four glutathione S-transferase (GST) genes from Mytilus galloprovincialis, Fish Shellfish Immunol. 34 (2013) 697–703, https://doi.org/10.1016/j.fsi.2012.11.020.

[64] C. Loguercio, N. Caporaso, C. Tuccillo, F. Morisco, G. Del Vecchio Blanco, C. Del Vecchio Blanco, Alpha-glutathione transferases in HCV-related chronic hepatitis: a new predictive index of response to interferon therapy? J. Hepatol. 28 (1998) 390–395, https://doi.org/10.1016/S0168-8278(98)80311-5.

[65] S.D.N.K. Bathige, N. Umasuthan, K. Saranya Revathy, Y. Lee, S. Kim, M.Y. Cho, M.A. Park, I. Whang, J. Lee, A mu class glutathione S-transferase from Manila clam Ruditapes philippinarum (RpGSTμ): cloning, mRNA expression, and conjugation assays, Comp. Biochem. Physiol. C Toxicol. Pharmacol. 162 (2014) 85–95, https://doi.org/10.1016/j.cbpc.2014.03.007.

[66] A.R. Abbas, D. Baldwin, Y. Ma, W. Ouyang, A. Gurney, F. Martin, S. Fong, M. van Lookeren Campagne, P. Godowski, P.M. Williams, A.C. Chan, H.F. Clark, Immune response in silico (IRIS): immune-specific genes identified from a compendium of microarray expression data, Genes Immun. 6 (2005) 319–331, https://doi.org/10.1038/sj.gene.6364173.

[67] D.T. Fearon, Identification of the membrane glycoprotein that is the C3b receptor of the human erythrocyte, polymorphonuclear leukocyte, B lymphocyte, and monocyte, J. Exp. Med. 152 (1980) 20–30.

[68] D. Morera, S.A. MacKenzie, Is there a direct role for erythrocytes in the immune response? Vet. Res. 42 (2011) 89, https://doi.org/10.1186/1297-9716-42-89.

[69] E. Nemeth, A.W. Baird, C. O'Farrelly, Microanatomy of the liver immune system, Semin. Immunopathol. 31 (2009) 333–343, https://doi.org/10.1007/s00281-009-0173-4.

[70] C. Erridge, E. Bennett-Guerrero, I.R. Poxton, Structure and function of lipopolysaccharides, Microb. Infect. 4 (2002) 837–851, https://doi.org/10.1016/S1286-4579(02)01604-0.

[71] S.O. Agriculture, Fish Diseases and Disorders ume 3 Viral , Bacterial and Fungal Infections, 1999.

[72] T. MIYAZAKI, N. KAIGE, Comparative histopathology of edwardsiellosis in fishes, Fish Pathol. 20 (1985) 219–227, https://doi.org/10.3147/jsfp.20.219.

[73] J.A. Robinson, F.P. Meyer, Streptococcal fish pathogen, J. Bacteriol. 92 (1966) 512 http://www.pubmedcentral.nih.gov/articlerender.

[74] M. Neely, J. Pfeifer, M. Caparon, Streptococcus-zebrafish model of bacterial pathogenesis, Infect. Immun. 70 (2002) 3904–3914, https://doi.org/10.1128/IAI.70.7.3904.

[75] M.F. Goody, E. Peterman, C. Sullivan, C.H. Kim, Quantification of the respiratory burst response as an indicator of innate immune health in zebrafish, J. Vis. Exp. (2013) 1–9, https://doi.org/10.3791/50667.

[76] A.E. Ellis, Innate host defense mechanisms of fish against viruses and bacteria, Dev. Comp. Immunol. 25 (2001) 827–839, https://doi.org/10.1016/S0145-305X(01)00038-6.

[77] J. Agramonte-Hevia, A. González-Arenas, D. Barrera, M. Velasco-Velázquez, Gram-negative bacteria and phagocytic cell interaction mediated by complement receptor 3, FEMS Immunol. Med. Microbiol. 34 (2002) 255–266 https://doi.org/10.1111/j.1574-695X.2002.tb00640.x.

[78] C.J. Secombes, T.C. Fletcher, The role of phagocytes in the protective mechanisms of fish, Annu. Rev. Fish Dis. 2 (1992) 53–71, https://doi.org/10.1016/0959-8030(92)90056-4.

[79] R.M. Day, Y.J. Suzuki, Cell proliferation, reactive oxygen and cellular glutathione, Dose Response 3 (2006) 425–442, https://doi.org/10.2203/dose-response.003.03.010.

[80] I.M. Dubovskiy, V. V Martemyanov, Y.L. Vorontsova, M.J. Rantala, E. V Gryzanova, V. V Glupov, Effect of bacterial infection on antioxidant activity and lipid peroxidation in the midgut of Galleria mellonella L. larvae (Lepidoptera, Pyralidae), Comp. Biochem. Physiol. C Toxicol. Pharmacol. 148 (2008) 1–5, https://doi.org/10.1016/j.cbpc.2008.02.003.

[81] D.P. Dixon, A. Lapthorn, R. Edwards, Plant glutathione transferases, Genome Biol. 3 (2002) REVIEWS3004.

[82] R. Edwards, D.P. Dixon, Plant glutathione transferases, Methods Enzymol. 401 (2005) 169–186, https://doi.org/10.1016/S0076-6879(05)01011-6.

[83] J.D. Hayes, D.J. Pulford, The glut athione S-transferase supergene family: regulation of GST and the contribution of the lsoenzymes to cancer chemoprotection and drug resistance Part I, Crit. Rev. Biochem. Mol. Biol. 30 (1995) 445–520, https://doi.org/10.3109/10409239509083491.

[84] B.Y. Kim, W.L. Hui, K.S. Lee, H. Wan, H.J. Yoon, Z.Z. Gui, S. Chen, B.R. Jin, Molecular cloning and oxidative stress response of a sigma-class glutathione S-transferase of the bumblebee Bombus ignitus, Comp. Biochem. Physiol. B Biochem. Mol. Biol. 158 (2011) 83–89, https://doi.org/10.1016/j.cbpb.2010.09.012.

[85] G. Arango Duque, A. Descoteaux, Macrophage cytokines: involvement in immunity and infectious diseases, Front. Immunol. 5 (2014) 491, https://doi.org/10.3389/fimmu.2014.00491.

[86] J.-M. Zhang, J. An, Cytokines, inflammation, and pain, Int. Anesthesiol. Clin. 45 (2007) 27–37, https://doi.org/10.1097/AIA.0b013e318034194e.

[87] J. Zou, C.J. Secombes, The function of fish cytokines, Biology (Basel) 5 (2016) 23, https://doi.org/10.3390/biology5020023.

[88] L. Romero, M.A. Higgins, J. Gilmore, K. Boudreau, A. Maslen, H.J. Barker, G.M. Kirby, Down-regulation of alpha class glutathione < /em &gt-Transferase by interleukin-1β in human intestinal epithelial cells (Caco-2) in culture, Drug Metab. Dispos. 30 (2002) 1186, https://doi.org/10.1124/dmd.30.11.1186 LP-1193.

[89] K. Maheo, J. Antras-Ferry, F. Morel, S. Langouët, A. Guillouzo, Modulation of glutathione S-transferase subunits A2, M1, and P1 expression by interleukin-1β in rat hepatocytes in primary culture, J. Biol. Chem. 272 (1997) 16125–16132, https://doi.org/10.1074/jbc.272.26.16125.

[90] E. Peterhans, Sendai virus stimulates chemiluminescence in mouse spleen cells, Biochem. Biophys. Res. Commun. 91 (1979) 383–392, https://doi.org/10.1016/0006-291X(79)90630-2.

[91] B. Mattle, A.B. Wilson, Body size preferences in the pot-bellied seahorse Hippocampus abdominalis: choosy males and indiscriminate females, Behav. Ecol. Sociobiol. 63 (2009) 1403–1410, https://doi.org/10.1007/s00265-009-0804-8.

[92] Yanhao Zhang, Haohan Zhang, Zhibin Zhang, et al., pH effect on heavy metal release from a polluted sediment, J. Chem. 2018 (2018) Article ID 7597640, 7 pages https://doi.org/10.1155/2018/7597640.

[93] B. Mannervik, P. Alin, C. Guthenberg, H. Jensson, M.K. Tahir, M. Warholm, H. Jörnvall, Identification of three classes of cytosolic glutathione transferase common to several mammalian species: correlation between structural data and enzymatic properties, Proc. Natl. Acad. Sci. U.S.A. 82 (1985) 7202–7206, https://doi.org/10.1073/pnas.82.21.7202.